Photoneutron studies of $E1$, $M1$, and $E2$ excitations in ^{13}C

R. J. Holt, R. M. Laszewski,* H. E. Jackson, J. E. Monahan, and J. R. Specht
Argonne National Laboratory, Argonne, Illinois 60439
(Received 26 November 1979)

The angular distribution for the $^{13}C(\gamma,n_0)^{12}C$ reaction was observed in the energy region 6.5 to 9.3 MeV and at angles of 90° and 135°. The photoneutron measurements were analyzed in terms of a multilevel R-matrix formalism. The $^{12}C(n,n)^{12}C$ reaction channel was explicitly included in this analysis. The effects of potential capture were directly observed in the photoneutron spectra. The ground-state radiative widths for resonances in this energy region were deduced from the R-matrix interpretation of the results. The ground-state transition probabilities for $E1$ excitations at 7.69 and 8.19 MeV were found to be in good agreement with the predictions of the weak-coupling model.

[NUCLEAR REACTIONS $^{13}C(\gamma,n_0)^{12}C$, $E_{exc}=6.5-9.3$ MeV, measured $\sigma(\theta)$, $\theta=90°$, 135°; deduced $\Gamma_{\gamma 0}$.]

I. INTRODUCTION

There have been numerous theoretical and experimental studies of low-lying levels in ^{13}C. The theoretical studies fall into two broad categories, the weak-coupling approach[1] and the more detailed shell-model calculations. The weak-coupling model[2-4] has been successful in describing the essential features of the $^{12}C(n,n)^{12}C$ reaction below a neutron energy of 5 MeV. The most notable of these calculations is the work of Lovas,[2] who used the Feshbach formalism and Reynolds *et al.*,[3] who used the coupled-channel approach of Tamura.[5] In fact, Reynolds *et al.* provided a detailed description of both the observed cross sections and polarizations in the $^{12}C+n$ system. Unfortunately, the studies of electromagnetic transition rates in the mass 13 system have not been as successful. These transition matrix elements have been computed using bound-state shell-model wave functions. Barker[6] used a weak-coupling approach, while Jäger *et al.*[7] took into account all 1 $\hbar\omega$ configurations. Kissener *et al.*[8] improved upon the work of Jäger *et al.* by incorporating into the bound-state calculation an R-matrix theory to account for nuclear decay. Of course, the most detailed calculation in the 1-p shell nuclei is that of Cohen and Kurath.[9] These models differ rather markedly on predictions of the strengths of low-lying $E1$ excitations. For example, for the 8.19-MeV $E1$ excitation in ^{13}C, the weak-coupling model[6] predicts a value which is an order of magnitude greater than that of the full shell-model calculations.[7]

Although there have been numerous experimental studies[10-13] of the $^{13}C(\gamma,n)^{12}C$ reaction, the values of the ground-state radiative widths for the $E1$ excitations at 7.69 and 8.19 MeV remain uncertain. The difficulties in extracting $\Gamma_{\gamma 0}$, unambiguously, in ^{13}C arise from the effects of large direct photoneutron reaction processes and a strong level-level interference. Moreover, these strong interference effects have led to the questionable speculation that there is a new resonance[12] in ^{13}C at 7.88 MeV.

Consequently, we observed the $^{13}C(\gamma,n_0)^{12}C$ cross section with high resolution in the photon energy range 6.5 to 9.3 MeV and at angles of 90° and 135°. The results were interpreted in terms of a multilevel R-matrix analysis which was developed specifically for photoneutron studies. The (n,n) reaction channel was explicitly included in the analysis so that the $^{12}C(n,n)^{12}C$ reaction was simultaneously described. The ground-state radiative widths for the $E2$ excitation at 7.56 MeV, the $E1$ resonances at 7.69 and 8.19 MeV, and the $M1$ resonance at 8.89 MeV were deduced from the analysis. It was found that the $E1$ excitations are reproduced remarkably well by the weak-coupling model.

II. EXPERIMENTAL METHOD

The differential cross section for the $^{13}C(\gamma,n_0)^{12}C$ reaction was measured using the photoneutron facility at the Argonne high-current electron Linac. The operating mode of the Linac was selected to produce 10.0-MeV electron bursts of 35-ps duration, 200-A peak current, and at a rate of 800 Hz. The electron pulses were converted to bremsstrahlung in a 0.15-cm thick Ag foil. The ^{13}C sample (90.7% enrichment) was irradiated with bremsstrahlung. The sample was in the form of powder and encased in a rectangular, thin-walled (0.8 mm

thick) Al holder of dimensions: 5.0-cm along the photon beam axis × 1.0-cm thick × 4.0-cm high. The photoneutrons traveled through two 11-m flight paths which were at angles of 90° and 135° with respect to the electron beam axis. The neutron energies were determined with high resolution (9.5 keV at $E_n = 1.5$ MeV and 34 keV at 4.0 MeV) using the time-of-flight method. The neutrons were detected in 2.5-cm thick NE110 plastic scintillation counters. The differential cross section was determined relative to the well-known cross section for the photodisintegration of the deuteron. The final cross sections are shown as the points in Fig. 1. The main features of the spectra are (1) a relatively large nonresonant cross section, (2) well-defined resonances at 7.56 and 8.89 MeV, and (3) a strong level-level interference pattern near 7.9 MeV. Except for the narrow resonance at 7.56 MeV, which was barely visible in the early photoneutron work,[10-13] the present observation at 90° is in excellent agreement with the previous measurements. Background effects were estimated by replacing the ^{13}C target with an identical ^{12}C sample. The background was found in this way to be <10% of the foreground at all energies. Since the first excited state in ^{12}C occurs at 4.44 MeV, there is no ambiguity associated with nonground-state neutron transitions in this work.

III. PHOTONEUTRON PROCESSES IN ^{13}C

The photoexcitation processes of ^{13}C are summarized in Fig. 2. An $E1$ photon can excite $\frac{1}{2}^+$ or $\frac{3}{2}^+$ resonances in ^{13}C. These levels subsequently decay by emitting an $s_{1/2}$ or $d_{3/2}$ neutron, respectively. An $M1$ photon excites $\frac{1}{2}^-$ or $\frac{3}{2}^-$ resonances which decay to the ground state of ^{12}C by $p_{1/2}$ or $p_{3/2}$ neutrons. $E2$ photoexcitations are $\frac{3}{2}^-$ or $\frac{5}{2}^-$ and decay by $p_{3/2}$ or $f_{5/2}$ neutrons. All of these photoexcitation processes are explicitly included in the analysis. No multipolarities of order higher than $E2$ were considered. This restriction simplifies the analysis since the $d_{5/2}$ and $f_{7/2}$ neutron channels are ruled out. We note that the well-known $E_n = 2.08$-MeV, $\frac{5}{2}^+$ resonance is absent from the present data since it would require an $E3$ or $M2$ photoexcitation. In the energy region of the present work, there are no known $\frac{1}{2}^+$ or $\frac{3}{2}^-$ resonances. However, the nonresonant components of the $s_{1/2}$ and $p_{3/2}$ amplitudes were retained in the analysis. The expression for the photoneutron differential cross section was determined from the table of Carr and Baglin[14]:

$$\begin{aligned}\frac{d\sigma}{d\Omega} = \frac{\lambda_\gamma^2}{16}\,&\{[2|U_{s_{1/2}}|^2+2|U_{p_{1/2}}|^2+4|U_{p_{3/2}}(M1)|^2+4|U_{p_{3/2}}(E2)|^2+4|U_{d_{3/2}}|^2+6|U_{f_{5/2}}|^2]\\&+\{U^*_{s_{1/2}}[4U_{p_{3/2}}(M1)-4U_{p_{1/2}}+6.928U_{p_{3/2}}(E2)]+U^*_{d_{3/2}}[4U_{p_{1/2}}-4U_{p_{3/2}}(M1)+1.386U_{p_{3/2}}(E2)+12.471U_{f_{5/2}}]\}\\&\times P_1(\cos\theta)\\&+\{-2|U_{d_{3/2}}|^2+U^*_{p_{3/2}}(M1)[-2U_{p_{3/2}}(M1)+6.928U_{p_{3/2}}(E2)-6.928U_{f_{5/2}}]\\&+U^*_{p_{1/2}}[-4U_{p_{3/2}}(M1)-6.928U_{p_{3/2}}(E2)+6.928U_{f_{5/2}}]+U^*_{p_{3/2}}(E2)[2U_{p_{3/2}}(E2)+1.714U_{f_{5/2}}]\\&+3.429|U_{f_{5/2}}|^2-4U^*_{s_{1/2}}U_{d_{3/2}}\}P_2(\cos\theta)\\&+\{U^*_{d_{3/2}}[-5.543U_{f_{5/2}}-8.314U_{p_{3/2}}(E2)]-6.928U^*_{s_{1/2}}U_{f_{5/2}}\}P_3(\cos\theta)\\&+[-3.429|U_{f_{5/2}}|^2-13.714U^*_{p_{3/2}}(E2)U_{f_{5/2}}]P_4(\cos\theta)),\end{aligned}\tag{1}$$

where $U_{lJ}(\mathfrak{m}\mathfrak{L})$ are the collision matrix elements for the (γ,n) channel. These matrix elements will be described in the following section.

IV. THE R-MATRIX ANALYSIS

The application of the R-matrix theory to photoneutron reactions was discussed in detail in Ref. 15. Only the elements essential to the present analysis will be discussed here. From Ref. 15, the collision matrix for the photoneutron reaction is given by

$$U^{(lJ\mathfrak{L})}_{\gamma n} = -ie^{-i\phi_l}\sum_{\lambda\mu}A_{\lambda\mu}\Gamma^{1/2}_{\lambda lJ}\Gamma^{1/2}_{\mu\gamma_f lJ}+\left(\frac{8\pi(\mathfrak{L}+1)}{\mathfrak{L}\hbar v_n}\right)^{1/2}\frac{k_\gamma^{\mathfrak{L}+1/2}}{(2\mathfrak{L}+1)!!}(2J+1)^{-1/2}\langle\Psi_{f(J_f)}||H^{\mathfrak{L}}||(I_l-e^{2i\delta_{lJ}}O_l)\varphi_{lJ}\rangle,\tag{2}$$

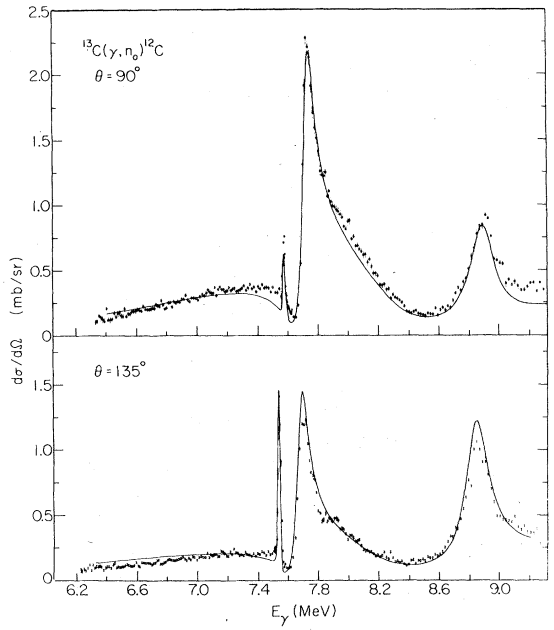

FIG. 1. High-resolution spectra for the $^{13}C(\gamma,n_0)^{12}C$ reaction at angles of 90° and 135°. The curves represent the results of an R-matrix analysis of the data.

where J is the spin of the excited state and J_f is the ground-state spin of ^{13}C in this case. The first term of Eq. (2) is due to internal capture or that component that arises from capture inside the channel radius. The second term is due to external capture. Outside the channel radius, the initial neutron-nucleus state is described by the scattering wave function. $H^{\mathcal{L}}$ is the electromagnetic operator for either $E1$, $M1$, or $E2$ radiation in the present case. The contribution from the external capture term is due to the long-range nature of the electromagnetic interaction. The δ_{lJ} are the phase shifts which describe the neutron-nucleus scattering. Since only the photon and neutron channels are

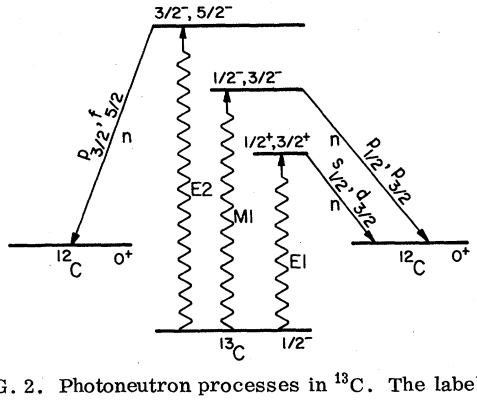

FIG. 2. Photoneutron processes in ^{13}C. The labels l_J on the neutron decay branch refer to the orbital angular momenta and total spins of the neutrons relative to the ^{12}C nucleus.

open in this energy range and since the neutron scattering cross section is $\gtrsim 10^3$ times greater than the photoneutron cross section, then Eq. (2) provides a complete representation of the photoneutron reaction.

The phase shifts were parametrized in terms of the R-function R_{lJ} in the following manner

$$\delta_{lJ} = -\phi_l + \tan^{-1}\{P_l R_{lJ}/[1 - R_{lJ}(S_l - b_{lJ})]\},$$

where ϕ_l, S_l, P_l, and b_{lJ} are the hard-sphere phase shifts, shift factors, penetration factors, and boundary condition constants, respectively. The R function is given by

$$R_{lj} = \sum_\lambda \frac{\gamma_{\lambda lJ}{}^2}{E_{\lambda lJ} - E} + R_{0lJ} + R_{1lJ}E\,,$$

where the last two terms describe the contributions from distant levels and $\gamma_{\lambda lJ}{}^2$ are the reduced widths. The most recent set of R-function parameters[16] were used in the present analysis. The results of this R-function analysis of Ref. 16 are in excellent agreement with the total cross section, angular distributions, and neutron polarizations below a neutron energy of 4 MeV. These parameters are summarized in Table I. The final state wave function $\Psi_{f(J_f)}$ in Eq. (2) was taken to be a Whittaker function

$$\Psi_{f(J_f)} = \left(\frac{2}{R}\right)^{1/2} \theta_{fc_f} \frac{W_{c_f}(k_f r)}{W_{c_f}(k_f R)}\, \varphi_c(J_f, M_f)\,,$$

where θ_{fc_f} is the reduced width of Lane and Thomas[17]

$$\theta_{fc_f} = \gamma_{fc_f}/(\hbar^2/MR^2)^{1/2}$$

and k_f is the wave number corresponding to the binding energy of the neutron in ^{13}C. The $\theta_{1/2^-}$ was adjusted in order to fit the observed photoneutron cross section. This quantity is defined by the amount of nonresonant potential capture in the $^{13}C(\gamma,n_0)^{12}C$ reaction.

We now focus attention on the internal capture

TABLE I. R-function parameters for the $^{12}C(n,n)^{12}C$ reaction and the present analysis. [Note that the $d_{5/2}$ and $f_{7/2}$ parameters are not necessary for the (γ,n) channel.] Channel radius, $R = 4.61$ fm.

l_J	$E_{\lambda lJ}$ (MeV)	$\gamma_{\lambda lJ}{}^2$ (MeV)	R_{0lJ}	R_{1lJ} (MeV^{-1})	b_{lJ}
$s_{1/2}$	−1.887	0.666	0.0245	0.0	0.0
$p_{1/2}$	4.20	0.080	0.09	0.05	−0.2
$p_{3/2}$	−1.267	0.050	0.261	0.05	−0.18
	4.940	0.010			
$d_{3/2}$	2.930	0.165	0.250	0.0	−1.0
	3.510	0.968			
$f_{5/2}$	2.810	0.006	0.0	0.0	−1.3

component in Eq. (2). The $\Gamma_{\lambda IJ}$ and $\Gamma_{\mu\gamma_f IJ}$ are the neutron width and internal capture width, respectively. $A_{\lambda\mu}$ is the transformation which relates the internal wave function to the real wave function for a given resonance.

$$(A^{-1})_{\lambda\mu} = (E_{\gamma\lambda} - E)\delta_{\lambda\mu} - \xi_{\lambda\mu} ,$$

where

$$\xi^{IJ}_{\lambda\mu} = \sum_c [(S_{I,c} - b_{IJ,c}) + iP_{I,c}]\gamma_{\lambda IJ,c}\gamma_{\mu IJ,c}$$

and the sum is taken over all reaction channels. The internal capture widths were determined by a least-squares fit to the data. The R-matrix analysis is compared with the observed differential cross section in Fig. 1. The data are well described by the R-matrix interpretation. The deduced parameters are given in Table II. The width for the $\frac{5}{2}^-$ level was chosen to be approximately $\frac{1}{10}$ of the energy resolution of the time-of-flight spectrometer. The width of this level is known[18] to be small and without question smaller than 2 keV. However, for the present work we wish to extract the ground-state radiative width $\Gamma_{\gamma 0}$ and no error is introduced by this arbitrary choice as long as it is much smaller than the resolution function. In order to obtain the curves in Fig. 1, a triangular resolution function was folded in with the R-matrix calculation. This resolution function has a large effect upon the 7.56 MeV resonance. The effect of the resolution broadening is insignificant for the remaining spectrum.

The parameters that were allowed to vary in the present analysis were the $(\Gamma_{n\lambda})^{1/2}$, $(\Gamma_{\gamma_f\lambda})^{1/2}$, and $\theta_{1/2^-}$. Although, in principle, the magnitude of $(\Gamma_{n\lambda})^{1/2}$ can be determined from the reduced widths in Table I, a better fit was obtained by allowing them to vary. In Table III these widths are compared with those obtained from R-function analyses[16,19] of neutron elastic scattering. The neutron widths were deduced from the reduced widths with the following expression

$$\Gamma_{n\lambda} = 2P_I(k_R R)\gamma_{\lambda n}{}^2 ,$$

where P_I is the penetration factor and k_R is the neutron wave number evaluated at the resonance energy. The widths for the $d_{3/2}$ resonances are in good agreement with the present work. However, the width of the $p_{1/2}$ level from Ref. 16 seems rather broad. Our result is in better agreement with the Yale R-function analysis[19] for that resonance. One possible explanation for this disagreement is that the R-function analysis of Ref. 16 was performed primarily for angular distribution data for the $^{12}C(n,n)^{12}C$ reaction below $E_n = 4$ MeV, whereas that of Ref. 19 and the present work extended to approximately 5 MeV.

TABLE II. R-matrix parameters for $^{13}C(\gamma,n_0)^{12}C$ reaction: $R = 4.61$ fm, $\theta_{1/2^-} = -0.524$.

$\mathcal{ML}$	J^π	$E_{\gamma\lambda}$ (MeV)	$(\Gamma_{n\lambda})^{1/2}$ $(\text{MeV})^{1/2}$	$(\Gamma_{\gamma_f\lambda})^{1/2}$ $(\text{eV})^{1/2}$
$E2$	$\frac{5}{2}^-$	7.534	0.045[a]	0.346
$E1$	$\frac{3}{2}^+$	7.636	0.412	2.068
$E1$	$\frac{3}{2}^+$	8.151	1.053	1.664
$M1$	$\frac{1}{2}^-$	8.861	0.412	−2.258
$E1$	$\frac{1}{2}^+$	11.000[b]	1.414	−2.966
$E1$	$\frac{3}{2}^+$	11.000[b]	1.414	−2.280

[a] This width was chosen to be 0.1 of the energy resolution spread at this energy.

[b] These resonances were arbitrarily placed here in order to account for the effects of distant levels.

TABLE III. Comparison of the values of Γ_n deduced from the present analysis with those from R-function analyses of elastic n-^{12}C scattering results.

E_γ (MeV)	J^π	Γ_n(MeV) Yale	ANL	Present work
7.69	$\frac{3}{2}^+$	0.15	0.15	0.17
8.19	$\frac{3}{2}^+$	1.11	1.15	1.11
8.89	$\frac{1}{2}^-$	0.20	0.24	0.17

V. RESULTS AND DISCUSSION

The collision matrix, Eq. (2), can be written in an equivalent manner in the level representation[15]

$$U^{(IJ\mathcal{L})}_{\gamma n} = -ie^{-i\phi_I}\sum_{\gamma\mu} A_{\lambda\mu}\Gamma_{\lambda n}{}^{1/2}[\Gamma_{\mu\gamma}{}^{1/2} + (\delta\Gamma_{\mu\gamma})^{1/2}]$$

$$+U_{\gamma n}(\text{HS}) ,$$

where $U_{\gamma n}(\text{HS})$ is the hard-sphere capture component. From the above expression it is clear that ground-state radiative widths depend upon both the internal capture width and the resonant component of external capture or the channel capture width $\delta\Gamma_{\gamma f}$. The amplitude for channel capture is given by the expression

$$(\delta\Gamma_{\gamma f})^{1/2} = \left[\frac{8\pi(\mathcal{L}+1)}{\mathcal{L}\hbar v_n}\right]^{1/2} \frac{k_\gamma^{\mathcal{L}+1/2}}{(2\mathcal{L}+1)!!}$$

$$\times e^{-i\phi_I}(2J+1)^{-1/2}$$

$$\times \Gamma_{\gamma n}{}^{1/2}\langle\Psi_{1/2^-}|\,||H^{(\mathcal{L})}||O_I\varphi_{I(J)}\rangle .$$

The way in which the integral in the above equation

TABLE IV. Deduced ground-state radiative widths for the $^{13}C(\gamma,n_0)^{12}C$ reaction.

E_γ (MeV)	$\mathfrak{M}\mathfrak{L}$	J^π	$\Gamma_{\gamma 0}$ (eV) Present work	Darmstadt
7.56	$E2$	$\frac{5}{2}^-$	0.11 ± 0.015	0.1150 ± 0.0062
7.69	$E1$	$\frac{3}{2}^+$	0.6 ± 0.1	
8.19	$E1$	$\frac{3}{2}^+$	7.0 ± 0.9	
8.89	$M1$	$\frac{1}{2}^-$	5.4 ± 0.5	3.36 ± 0.46

is computed was given in the Appendix of Ref. 15 and will not be discussed further. Then $\Gamma_{\gamma 0}$ is given by

$$\Gamma_{\gamma 0} \equiv \left| \Gamma_{\gamma f}^{1/2} + (\delta\Gamma_{\gamma f})^{1/2} \right|^2 .$$

This $\Gamma_{\gamma 0}$ is the quantity[20] that would be determined from a traditional area analysis of the data, i.e., this $\Gamma_{\gamma 0}$ governs the peak height of the resonance in the (γ,n) cross section. The final results are given in Table IV. For the 7.56-MeV, $E2$ excitation, we have extremely good agreement with the inelastic electron scattering results.[21] However, for the 8.89-MeV $M1$ excitation, the results of the present experiment disagree with the Darmstadt value[21] for the $M1$ component of the transition strength. The errors in our experimental values of $\Gamma_{\gamma 0}$ were estimated by taking extreme cases for the effects of distant levels in the (γ,n) channel. In addition, we fixed the Darmstadt value for $\Gamma_{\gamma 0}$ for the $M1$ excitation in our analysis and readjusted all the other parameters. We found no combination of the other parameters that would give a reasonable fit to the photoneutron cross sections. The origin of this discrepancy remains unknown. However, in the inelastic electron scattering process, the $\frac{1}{2}^-$ resonance can be excited by both $E0$ and $M1$ transitions. Unfortunately, in Ref. 21 there was no discussion of the method for unraveling the $M1$ radiative width from the $E0$ transition rate.

The deduced $\Gamma_{\gamma 0}$ are compared with theoretical predictions in Table V. The results for the $E1$ excitations are in remarkably good agreement with the early calculations of Barker[6] and in disagreement with the recent shell-model calculations of Jäger *et al.*[7] and Kissener *et al.*[8] Kurath[22] predicted the total strength for these two resonances and the results are in fair agreement with the present measurement. The Cohen-Kurath results overestimate the $M1$ transition rate for the 8.89-MeV resonance, but they are in fair agreement with the $E2$ transition.

It is surprising that the more detailed models underestimate the amount of $E1$ strength in the 7.69- and 8.19-MeV resonances. This present work provides additional evidence that the essential features of these resonances can be explained in terms of the weak-coupling model. This result was suggested in the work of Fukuda,[11] but the observed strength for the lower energy resonance was more than five times greater than the present observation. Of course, this is the magnitude of discrepancy one would expect from a traditional area analysis of these strongly interfering resonances.

It is noteworthy that the Lane reduced width for $^{12}C+n$, $\theta_{1/2^-}=-0.524$, is near the value obtained[15] for $^{16}O+n$, $\theta_{5/2^+}=-0.59$. This implies that ^{13}C is nearly as well represented as a ^{12}C core plus a neutron as ^{17}O can be described by a ^{16}O core and a neutron.

VI. CONCLUSIONS

The differential cross section for the $^{13}C(\gamma,n_0)^{12}C$ reaction was measured with high resolution throughout the photon energy range 6.5 to 9.3 MeV. These results were interpreted in terms of a multilevel, multichannel R-matrix analysis and the ground-state widths were extracted. The $\Gamma_{\gamma 0}$ of the $E2$ resonance at 7.56 MeV was found to agree well with the inelastic electron scattering results, while that of the $M1$ resonance at 8.89 MeV does not agree. The radiative widths for the two strongly interfering $E1$ excitations at 7.69 and 8.19 MeV were found to be in excellent agreement

TABLE V. Comparison of the deduced internal capture widths with theoretical predictions.

E_γ (MeV)	$\mathfrak{M}\mathfrak{L}$	Present experiment	$\Gamma_{\gamma 0}$ (eV) Barker	Jäger *et al.*	Kissener *et al.*	Kurath[a]
7.56	$E2$	0.11 ± 0.015				0.18
7.69	$E1$	0.6 ± 0.1	0.71	0.60	1.54	3.78[b]
8.19	$E1$	7.0 ± 0.9	5.49	0.53	0.89	
8.89	$M1$	5.4 ± 0.5			6.13	13.87–14.78

[a]References 9 and 22.

[b]Only the integrated strength from both $E1$ excitations is quoted.

with predictions of a weak-coupling model, while the strength of the 8.19-MeV resonance is in clear disagreement with the more sophisticated shell-model calculations. The direct component of the interaction was found to be large, indicating a need for calculations which include the single-particle nature of ^{13}C.

This research was performed under the auspices of the United States Department of Energy.

---

*Present address: Department of Physics, University of Illinois, Urbana-Champaign, Illinois 61801.

[1]A. M. Lane, Rev. Mod. Phys. 32, 519 (1960).
[2]I. Lovas, Nucl. Phys. 81, 353 (1966).
[3]J. T. Reynolds, C. T. Slavik, C. R. Lubitz, and N. C. Francis, Phys. Rev. 176, 1213 (1968).
[4]J. E. Purcell and M. R. Meder, Phys. Rev. C 16, 76 (1977).
[5]T. Tamura, Rev. Mod. Phys. 37, 679 (1965).
[6]F. C. Barker, Nucl. Phys. 28, 96 (1961).
[7]H. U. Jäger, H. R. Kissener, and R. A. Eramzhian, Nucl. Phys. A171, 16 (1971).
[8]H. R. Kissener, A. Asward, R. A. Eramzhian, and H. U. Jäger, Nucl. Phys. A219, 601 (1974).
[9]S. Cohen and D. Kurath, Nucl. Phys. 73, 1 (1965).
[10]W. Bertozzi, P. T. Demos, S. Kowalski, F. R. Paolini, C. P. Sargent, and W. Turchinetz, Nucl. Instrum. Methods 33, 199 (1965).
[11]K. Fukuda, Nucl. Phys. A156, 10 (1970).
[12]J. G. Woodworth, K. G. McNeill, J. W. Jury, P. D. Georgopulos, and R. G. Johnson, Can. J. Phys. 55, 1704 (1977).
[13]J. G. Woodworth, K. G. McNeil, J. W. Jury, R. A. Alvarez, B. L. Berman, D. D. Faul, and P. Meyer, Phys. Rev. C 19, 1667 (1979).
[14]R. W. Carr and J. E. Baglin, Nucl. Data Tables 10, 143 (1971).
[15]R. J. Holt, H. E. Jackson, R. M. Laszewski, J. E. Monahan, and J. R. Specht, Phys. Rev. C 18, 1962 (1978).
[16]A. Smith, R. Holt, and J. Whalen, Nucl. Sci. Eng. 70, 281 (1979).
[17]A. M. Lane and R. G. Thomas, Rev. Mod. Phys. 30, 257 (1958).
[18]S. Cierjacks, P. Forti, D. Kopsch, L. Kropp, J. Nebe, and H. Unfeld, Kernforschungszentrum Karlsruhe Report No. KFK-1000, 1968.
[19]R. J. Holt, F. W. K. Firk, R. Nath, and H. L. Schultz, Nucl. Phys. A213, 147 (1973).
[20]Note that this definition differs slightly from that of Ref. 15, since the expression for internal capture in Eq. (2) differs by a minus sign from that of Ref. 15.
[21]G. Wittwer, H.-G. Clerc, and G. A. Beer, Phys. Lett. 30B, 634 (1969).
[22]D. Kurath, private communication.